

SINGLE-STRUCTURE 3-AXIS LORENTZ FORCE MAGNETOMETER WITH SUB-30 nT/ $\sqrt{\text{HZ}}$ RESOLUTION

Mo Li¹, Eldwin J. Ng², Vu A. Hong², Chae H. Ahn², Yushi Yang²,
Thomas W. Kenny² and David A. Horsley¹

¹University of California, Davis, USA

²Stanford University, USA

ABSTRACT

This work demonstrates a 3-axis Lorentz force magnetometer for electronic compass purposes. The magnetometer measures magnetic flux in 3 axes using a single structure. With 1 mW power consumption, the sensor achieves sub-30 nT/ $\sqrt{\text{Hz}}$ resolution in each of the 3 axes. Compared to the 3-axis Hall sensors currently used in smartphones, the 3-axis magnetometer shown here has the advantages of 10 \times lower noise floor and the ability to be co-fabricated with MEMS inertial sensors.

INTRODUCTION

Unlike Hall-effect or magnetoresistive sensors, a Lorentz force magnetometer is a force sensor and typically operates at its mechanical resonance, f_n . The sensitivity of the sensor is directly proportional to the bias current flowing through the structure and to the length through which the current travels ($F_L = Li \times B$). One type of Lorentz force magnetometer modulates a low-frequency magnetic field up to f_n [1-3], thus the motion resulting from the Lorentz force is amplified by the mechanical quality factor (Q). Closed-loop operation of this type of sensor has also been demonstrated [4]. Another type of Lorentz force magnetometer has a frequency output; magnetic field is measured by monitoring the change in f_n as Lorentz force changes the stiffness of the resonator. In both types of magnetometers, it is desirable to have a larger bias current and longer current-carrying beam to improve the sensitivity and resolution of the sensor. Moreover, having high Q is always desirable for resonant sensors, as it improves the signal to noise ratio (SNR).

Multi-axis sensing and sensor integration is the trend of MEMS inertial sensors as they allow chip size and fabrication cost to be reduced while maintaining the same performance and reliability. Single-structure 3-axis gyroscopes are currently in full production and have been widely used in smart phones and portable devices [5]. Single-structure 3-axis accelerometers have also been demonstrated [6] whereas single-structure 3-axis magnetometers have not. Moreover, the lowest noise floor achieved in a MEMS Lorentz force magnetometer, fabricated in a process that requires electrically-isolated metal layers on top of the silicon MEMS structure, was reported as 70 nT/ $\sqrt{\text{Hz}}$ for z-axis field and 10 nT/ $\sqrt{\text{Hz}}$ for x-/y- axis field [7]. Most other Lorentz force magnetometers have noise levels greater than 200 nT/ $\sqrt{\text{Hz}}$. Here, we demonstrate a single-structure 3-axis Lorentz force magnetometer for electronic compass purposes, which has a noise floor below 30 nT/ $\sqrt{\text{Hz}}$. The magnetometer is fabricated in the epi-seal

process developed at Stanford University [8]. The process is currently used for high-volume manufacturing of micromechanical oscillators for timing applications by SiTime Inc. and provides a very low operating pressure (1 Pa). Pressure sensors, thermometers, accelerometers, gyroscopes [9] and magnetometers have been demonstrated using the same fabrication process. The magnetometer presented in this work is fully compatible with production MEMS processes such as the STMicroelectronics THELMA process and the Bosch's surface micromachining process, and can be fabricated on the same die with accelerometers and gyroscopes.

DESIGN

The 3-axis magnetometer consists of a 1.8 \times 1.8 mm² resonator fabricated in 40 μm thick (100) single-crystal silicon and wafer-level vacuum sealed at less than 1 Pa to reduce damping and increase quality factor (Q). An n-type wafer with doping level of 6E19 cm⁻³ (resistivity 1m Ω ·cm) is used to reduce the resistance of the current-carrying flexure. Figure 1 shows the schematic view and SEM image (inset) of the magnetometer. The structure is long to maximize Lorentz force, while the area is optimized to only 0.72 mm² (18% of the 2 \times 2 mm² die area). During operation, an ac bias current at a frequency close to f_n is injected through the structure which generates Lorentz force and therefore movement of the structure in the presence of magnetic field.

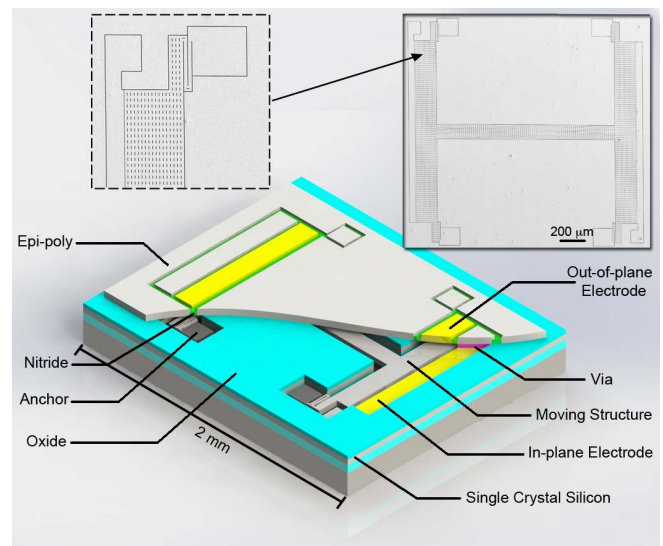


Figure 1: 3-axis Lorentz force magnetometer. Inset: SEM image of the magnetometer before epitaxial sealing process.

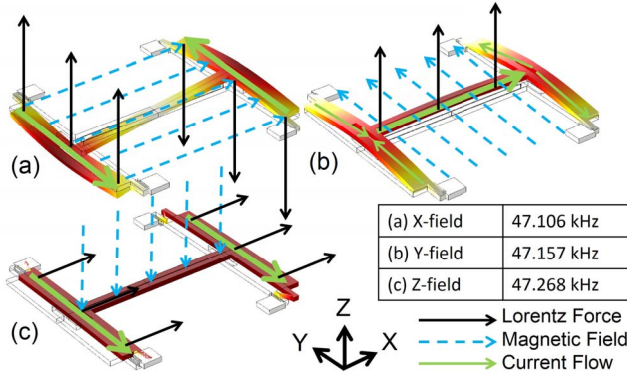


Figure 2: FEM simulation of the magnetometer. The excitation current (green arrows) is modulated at the resonance frequency, and low frequency magnetic field (blue dashed arrows) generates Lorentz force (black arrows) near the resonance frequency.

Multi-Axis Resonator

Figure 2 shows the FEM simulation of the three resonant modes excited by x , y and z field, with a detailed schematic of current flow and Lorentz force direction. Time-multiplexing is used to measure each axis of magnetic field in sequence by switching the direction of current flow. While time-multiplexing reduces the measurement bandwidth, cross-axis coupling is greatly reduced.

The three resonant frequencies were designed to be close to each other, so that when operating in open loop, only one frequency reference is required for 3-axis sensing. With the trade-off of reducing sensitivity, the bandwidth can be greatly enhanced by operating at a frequency slightly off-resonance [10]. The magnetometer can also be operated in closed-loop, providing the maximum sensitivity and at the same time better stability over temperature. The closed-loop operation also reduces the effect of self-heating due to the bias current, which would otherwise reduce the sensitivity because of the change in the natural frequency.

Capacitive Sensing

Capacitive pick-offs are used for displacement sensing, as illustrated in Figure 3. In-plane motion (z -axis field) is measured with a pair of differential parallel plates (C_{x+} and C_{x-}), while out-of-plane motion (x - or y - axis field) is measured by taking the difference (x -axis field) or sum (y -axis field) of the signals from two out-of-plane sense pick-offs (C_{z+} and C_{z-}) located above the moving structure. The electrode configurations for each axis are different, further reducing cross-axis coupling.

When designing the capacitive pick-offs, damping has to be considered. For typical micromechanical resonators with capacitive sensing, squeeze film gas damping and slide film gas damping dominate the damping for pressure levels down to 10-100 Pa [11]. Large sensing capacitance requires more die area and increases both damping and thermomechanical noise, however too little sensing capacitance causes electronic noise to dominate. Comb-finger and parallel plate

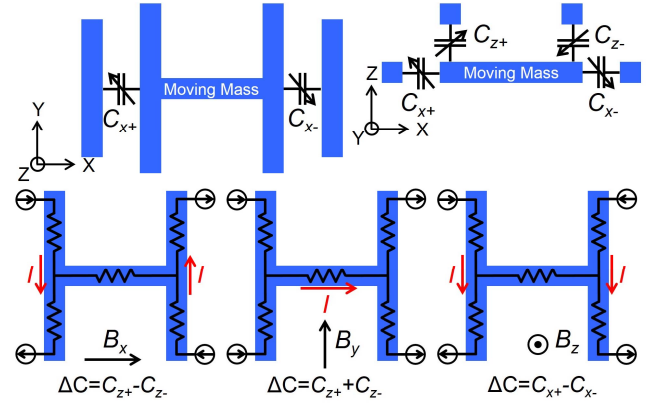


Figure 3: Capacitive pick-off placement for in-plane motion sensing (top left) and out-of-plane motion sensing (top right). Bottom schematics show the electrode configurations for x , y , and z axis magnetic field sensing.

capacitors are the most commonly used capacitive sensing types. Compared to comb-finger, parallel plate capacitive sensing gives larger sensitivity for the same area but also introduces transduction nonlinearity and electrostatic nonlinearity. However, for the full-range of Earth's field detection, the displacement resulting from Lorentz force is on the order of 1 nm and the nonlinearity from the parallel plate can be neglected. We considered device size, capacitance sensitivity, sensor's resolution and quality factor (Q) during the sensor design. The designed displacement-to-capacitance sensitivity is $\sim 1 \mu\text{F}/\text{m}$ in each axis.

RESULTS

Lorentz force bias current generating circuitry and capacitive sensing circuitry are implemented with discrete components on a PCB. We currently use 4 switches to manually select the sensing axis by setting the current flow direction, however this switching can be automated in the future. During operation, a $5.8 \text{ mA}_{\text{rms}}$ bias current is injected through the MEMS sensor. This Lorentz force bias current passes through a resistance of $\sim 30 \Omega$ in each axis, which results in a power consumption of 1 mW. A dc bias voltage is also applied to the moving mass at the same time for capacitive sensing. The Lorentz force results in a change in capacitance that is measured by a transimpedance amplifier. The measured electronic noise floor is $0.03 \text{ aF}/\sqrt{\text{Hz}}$ with a 4 V DC bias. A digital lock-in amplifier (Zurich Instruments HF2-LI) is used to generate the bias current at sensor's resonant frequency and demodulate the signal. Table I summarizes the magnetometer parameters for each axis.

Frequency Response and Sensitivity

Figure 4 shows measured frequency responses (left) and capacitance change vs. input magnetic field (right). Note here that the measured z -axis frequency response (in-plane resonating mode) shows that the resonance frequency is 2 kHz higher than the expected value from FEM simulation,

Table 1. Sensor Parameters

Parameter	X-field	Y-field	Z-field
Natural Frequency	47.43 kHz	47.29 kHz	49.10 kHz
Q	7100	3200	12700
Bandwidth	3.3 Hz	7.4 Hz	1.9 Hz
Power	1 mW	1 mW	1 mW
Sense Cap.	1947 fF	1947 fF	990 fF
Sense Gap	2 μm	2 μm	1 μm
Sensitivity	17.44 pF/T	9.28 pF/T	24.2 pF/T
Resolution	19 nT/ $\sqrt{\text{Hz}}$	32 nT/ $\sqrt{\text{Hz}}$	17 nT/ $\sqrt{\text{Hz}}$

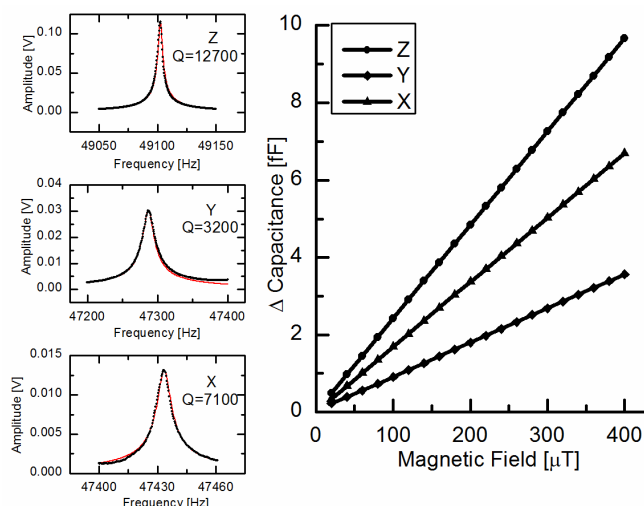


Figure 4: Frequency responses (left) and measured capacitance change vs. input magnetic field (right). The magnetometer is linear up to 400 μT in all three axes.

mainly due to the overcompensation for over-etch in the device layout. Although all three axes have similar 1 $\mu\text{F}/\text{m}$ displacement-to-capacitance sensitivities, they have different field-to-capacitance sensitivities due to different Q , an effect which can be compensated by the detection electronics. The difference in Q also results in slightly different thermomechanical noise-limited resolution. The magnetometer is linear (<1% nonlinearity) up to 400 μT in all three axes limited by the measurement setup.

Earth's Field Measurement

We use a commercial geomagnetometer (Integrity Design & Research IDR-321) to measure the Earth's field in our lab (Davis, California) as a reference (13 μT). To demonstrate that the MEMS magnetometer is capable of measuring Earth's field, the device is rotated 360° about its y-axis and the horizontal component of Earth's field is measured from the sensor's x- and z-axis outputs, showing

the expected $\sin(\theta)$ and $\cos(\theta)$ dependency in Figure 5. This measurement was performed with the magnetometer excited slightly off-resonance ($\Delta f_x = 7.2$ Hz, $\Delta f_z = 4.2$ Hz), trading sensitivity for increased bandwidth ($BW_x = 12$ Hz, $BW_z = 6.8$ Hz) and reduced sensitivity to temperature, similar to an approach recently proposed for gyroscopes [12]. Since the Brownian (thermomechanical) noise is at least 10× larger than the electronic noise floor, the resolution is not sacrificed by operating off-resonance [10].

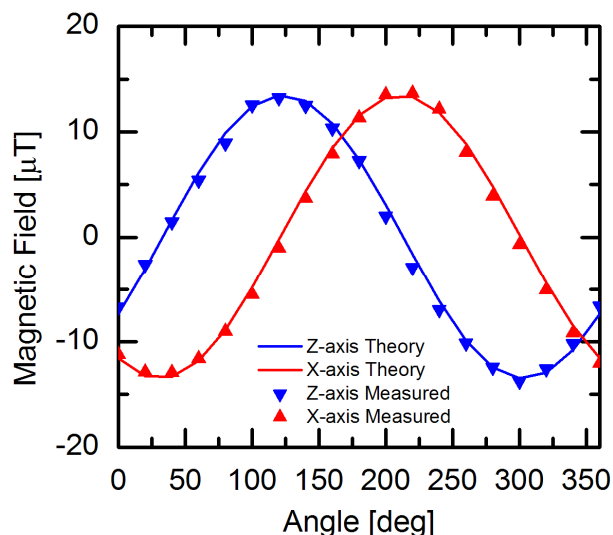


Figure 5: Magnetometer's response to the horizontal component of Earth's field (13 μT).

Cross-axis Sensitivity

The cross-axis sensitivity is measured by mounting the magnetometer inside a 2-axis Helmholtz coil. The accuracy of the measurement is limited by the accuracy of the alignment in our measurement setup (tens to hundreds of millidegrees). Note that a one-degree misalignment between the coil and the magnetometer introduces a -35 dB error in the cross-axis sensitivity.

Table 2 shows the measured cross-axis sensitivity. The low cross-axis sensitivity results from using (a) three different resonating modes, (b) time-multiplexing and (c) three different capacitive sensing configurations. The y-axis output shows larger coupling from the x-axis input compared to other combinations. This is possibly because a voltage source rather than a current source is used to provide the Lorentz force bias current. A resistance-mismatch in the current-carrying flexure due to fabrication variation results in a mismatch of the bias current. The mismatched bias current is orthogonal with the original bias current, which increases

Table 2. Measured Cross-axis Sensitivity

Input	X-OUT	Y-OUT	Z-OUT
X	0 dB	-29 dB	-65 dB
Y	-37 dB	0 dB	-63 dB
Z	-43 dB	-36 dB	0 dB

the cross-axis sensitivity. This effect can be suppressed by using a current source instead of voltage source.

Figure 6 compares the performance of recently reported MEMS Lorentz force magnetometers which are capacitively transduced. For both sensitivity and resolution, the bias current for Lorentz force generation is normalized to 1 mA for comparison. Kynäräinen's [7] torsional magnetometer and double-ended-tuning-fork magnetometer keep the record for sensitivity and resolution thanks to the electrically-isolated metal layer on the silicon MEMS structure, which increases the effective length of the current carrying beam by a factor of 5X-65X.

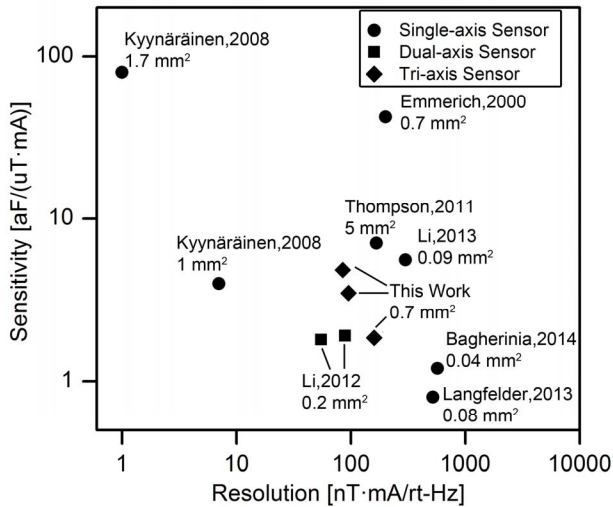


Figure 6: Comparison of capacitance sensitivity versus resolution of recently reported MEMS Lorentz force magnetometers.

CONCLUSION

We demonstrate a 3-axis Lorentz force magnetometer in a single structure. By optimizing the mechanical design, it achieves sub-30 nT/ $\sqrt{\text{Hz}}$ resolution for all three axes. Experimental results verify that the device is capable of measuring Earth's field. The cross-axis sensitivity is reduced by both mechanical design and time-multiplexing operation. Compared to previous single-axis and dual-axis magnetometers, the 3-axis magnetometer demonstrated in this work provides very good performance considering resolution, sensitivity and sensor size.

ACKNOWLEDGEMENTS

This work was supported by the Defense Advanced Research Projects Agency (DARPA) Precision Navigation and Timing program (PNT) managed by Dr. Andrei Shkel and Dr. Robert Lutwak under contract # N66001-12-1-4260 and the National Science Foundation under award number CMMI-0846379. The work was performed in part at the Stanford Nanofabrication Facility (SNF) which is supported by National Science Foundation through the NNIN under Grant ECS-9731293. The authors would also like to thank the SNF staff, particularly M. M. Stevens for the timely

assistance with the epitaxial reactor.

REFERENCES

- [1] L. M. Miller, J. A. Podosek, E. Kruglick, *et al.*, "A μ -magnetometer based on electron tunneling," in *IEEE MEMS*, 1996, pp. 467-472.
- [2] G. Langfelder, C. Buffa, A. Frangi, *et al.*, "Z-Axis Magnetometers for MEMS Inertial Measurement Units Using an Industrial Process," *Industrial Electronics, IEEE Transactions on*, vol. 60, pp. 3983-3990, 2013.
- [3] M. Li, V. T. Rouf, M. J. Thompson, *et al.*, "Three-Axis Lorentz-Force Magnetic Sensor for Electronic Compass Applications," *Microelectromechanical Systems, Journal of*, vol. 21, pp. 1002-1010, 2012.
- [4] M. Li, E. J. Ng, V. A. Hong, *et al.*, "Lorentz force magnetometer using a micromechanical oscillator," *Applied Physics Letters*, vol. 103, 173504, 2013.
- [5] B. Vigna, "It Makes Sense: How Extreme Analog and Sensing Will Change the World," in *Tech. Digest 2012 Solid-State Sensors, Actuators and Microsystems Workshop*, Hilton Head, SC, 2012, pp. 58-65.
- [6] M. A. Lemkin, B. E. Boser, D. Auslander, *et al.*, "A 3-axis force balanced accelerometer using a single proof-mass," in *Solid State Sensors and Actuators*, , 1997, vol. 2, pp. 1185-1188.
- [7] J. Kynäräinen, J. Saarilahti, H. Kattelus, *et al.*, "A 3D micromechanical compass," *Sensors and Actuators A: Physical*, vol. 142, pp. 561-568, 2008.
- [8] R. N. Candler, M. A. Hopcroft, B. Kim, *et al.*, "Long-Term and Accelerated Life Testing of a Novel Single-Wafer Vacuum Encapsulation for MEMS Resonators," *Microelectromechanical Systems, Journal of*, vol. 15, pp. 1446-1456, 2006.
- [9] S. Nitzan, C. H. Ahn, T. H. Su, *et al.*, "Epitaxially-encapsulated polysilicon disk resonator gyroscope," in *Micro Electro Mechanical Systems (MEMS), 2013 IEEE 26th International Conference on*, 2013, pp. 625-628.
- [10] G. Langfelder and A. Tocchio, "On the operation of Lorentz-force MEMS magnetometers with a frequency offset between driving current and mechanical resonance," *Magnetics, IEEE Transactions on*, vol. PP, pp. 1-6, 2013.
- [11] M.-H. Bao, *Analysis and design principles of MEMS devices* (Amsterdam: Elsevier).
- [12] M. W. Judy, J. A. Geen, and H. Johari-Galle, "Non-Degenerate Mode MEMS Gyroscope," US Patent 20120137774, 2012.

CONTACT

*Mo Li, tel: +1-530-752-5180; moxli@ucdavis.edu